

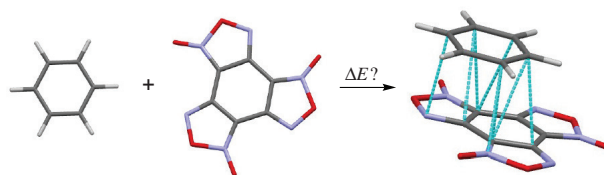
## Structure and complexation energy of benzotrifuroxan–benzene molecular complex

Dmitry V. Khakimov,\* Ivan D. Nesterov and Tatyana S. Pivina

N. D. Zelinsky Institute of Organic Chemistry, Russian Academy of Sciences, 119991 Moscow, Russian Federation. E-mail: 7933765@mail.ru

DOI: 10.1016/j.mencom.2021.03.017

Based on a combination of quantum chemistry and atom–atom potentials methods, we developed a technique for modeling the structure and estimating the complexation energy of a binary organic complex in gas and crystal phases. The efficiency of this technique was illustrated by an example of the benzotrifuroxan–benzene molecular complex. For both phases, the same molecular binary structure ( $\pi$ -stacking) was obtained with a parallel arrangement of the planes of BTF and benzene molecules and complexation energies of  $-11.9$  and  $-11.7$  kcal mol $^{-1}$  for a gas phase and a crystal cluster, respectively.



**Keywords:** bimolecular complex, cocrystal, atom–atom potentials method, DFT, global optimization, crystal structure, potential energy surface, complexation energy, benzotrifuroxan, benzene.

The creation of the cocrystal forms of physiologically active<sup>1,2</sup> and high-energy compounds<sup>3–6</sup> is a problem of considerable current interest. The main characteristic of cocrystals (and bimolecular forms in general) is the complexation energy ( $\Delta E$ ), and its estimation requires structure modeling in such a way that the resulting geometry corresponds to the global minimum of a potential energy surface (PES). For molecular clusters based on weak non-covalent interactions, the complex landscape of a PES and a large number of degrees of freedom make the problem of global optimization<sup>7</sup> of the structure rather nontrivial. The approaches to its solution include a basin-hopping method,<sup>8</sup> genetic algorithms,<sup>9,10</sup> etc.<sup>11</sup> A common feature of these approaches is their stochastic nature, and, as a consequence, they not always give a global solution. On the other hand, some approaches<sup>12</sup> (deterministic global optimization) allow one to confidently find a global minimum as a result of the complete screening of PES, although they are usually too expensive in actual practice in terms of computational resources.

In principle, the relative simplicity of bimolecular forms allows one to perform a systematic search for the global minimum on PES, provided that the energy evaluations and local optimizations would be fast enough. At the same time, the high speed calculations of energy and, as a consequence, the possibly approximate nature of its values can lead to an erroneous gradation of the energy of local minimums and an incorrect choice of the global one. To overcome this difficulty, a two-stage approach is widely used, in which the structures with a minimum energy found at the first stage of an approximate global search are then locally re-optimized on an appropriate *ab initio* or DFT level.

The aim of this study was to test such a two-stage approach in modeling the structure and evaluating the complexation energy of organic bimolecular complexes for gas and crystal phases using (1) the atom–atom potentials (AAP)<sup>13</sup> method in

deterministic global optimization and (2) DFT with a dispersion correction for the structure and energy refinement of the optimal system configurations found in the first step. A complex of benzotrifuroxan with benzene (BTF–PhH) was chosen for testing the proposed AAP–DFT technique because it consists of simple symmetric molecules, including BTF (a high-energy compound). Moreover, this complex has an experimental base.<sup>14</sup>

According to the AAP method, the intermolecular potential  $U$  is the sum of the potentials  $U_{ij}$  of pair interactions of each atom  $i$  of one molecule with each atom  $j$  of another. In our version of the method, atoms are considered as point charges, each placed at respective nuclei position in a molecule. The pairwise interatomic potential  $U_{ij}$  is represented as the sum of Coulomb ( $V_{ij}$ ) and van der Waals ( $W_{ij}$ ) terms

$$U_{ij} = V_{ij} + W_{ij} = \frac{q_i q_j}{r_{ij}} + \left\{ -\frac{A_{ij}}{r_{ij}^6} + B_{ij} e^{-\alpha_{ij} r_{ij}} \right\}, \quad (1)$$

where  $A_{ij}$ ,  $B_{ij}$  and  $\alpha_{ij}$  are empirical parameters of the Buckingham potential, determined by the atoms  $i$  and  $j$  involved in the interaction;  $q_i$  and  $q_j$  are atomic charges, and  $r_{ij}$  is the distance between the atoms  $i$  and  $j$ . Thus, for the isolated bimolecular complex BTF–PhH, the intermolecular potential  $U_{\text{BTF–PhH}}$  – a subject of the subsequent minimization – is defined as

$$U_{\text{BTF–PhH}} = \sum_{i \in \text{BTF}} \sum_{j \in \text{PhH}} U_{ij}, \quad (2)$$

where  $i$  and  $j$  run over all atoms in BTF and benzene molecules, respectively. It is clear that, in such an AAP approximation, the energy of complex formation  $\Delta E_{\text{AAP}}$  coincides with the intermolecular potential  $U$ , the former taking into account only electrostatic (ES) and van der Waals (vdW) interactions.

The actual atomic charges and intrinsic geometries of individual molecules in the complex are extracted from the data of preliminary quantum-chemical calculations. The atomic

charges are selected in such a way that the electrostatic potential of a system of the point charges simulating a molecule differs as little as possible (in the root mean square sense) from the real (quantum-chemical) molecular electrostatic potential (MEP) outside the van der Waals surface of the molecule.<sup>15</sup> In this work, the optimal geometries and MEPs of isolated BTF and benzene components were calculated at the B3LYP/6-31G(d,p) level using Gaussian 09.<sup>16</sup> The point charges were then fitted to MEPs using the FitMEP<sup>15</sup> program. The empirical parameters of the Buckingham potentials ( $A_{ab}$ ,  $B_{ab}$  and  $\alpha_{ab}$ ) were taken from the FIT<sup>17</sup> database. At this point, the analytical form of the intermolecular potential  $U$  and all necessary parameters for its minimization were defined.

A simple reliable strategy for deterministic global optimization implemented in the PMC<sup>18</sup> program was further applied. For this purpose, in the space group  $P1$ , a cubic cell was created with an initial size of  $(10 \times 10 \times 10) \text{ \AA}^3$ , into which BTF and benzene molecules were placed. The external environment (the periodicity of the crystal structure) was turned off. A number of starting models of the binary complex were formed in such a way as to be evenly distributed in a configuration space large enough to contain all possible minima. Both molecules forming the complex were represented as solids, and the position and spatial orientation of each molecule relative to the cell were determined by the fractional coordinates ( $a_i$ ,  $b_i$ ,  $c_i$ ) of the  $i$ th ( $i = 1, 2$ ) center of mass (COM) for the molecule and the corresponding Euler angles ( $\varphi_i$ ,  $\theta_i$ ,  $\psi_i$ ). Their coordinates combined for both molecules make up a 12-dimensional configuration space ( $a_1, b_1, c_1, \varphi_1, \theta_1, \psi_1, a_2, b_2, c_2, \varphi_2, \theta_2, \psi_2$ ) of the complex. While the position of a molecule (PhH) in the cube is fixed (e.g.,  $a_1, b_1$  and  $c_1$  are constants), the remaining nine coordinates are varied with a step of 1/4 for fractional coordinates of the other molecule's COM and  $30^\circ$  for the six Euler angles, yielding a variety of configurations with their number bounded from above by  $\sim 65 \times 10^6$ . A great part of possible configurations is skipped or rejected during the process,<sup>19</sup> namely, those equivalent to already generated ones due to the intrinsic symmetry of molecule(s) ( $C_{3h}$  for BTF and  $D_{6h}$  for benzene) or containing abnormally short intermolecular contacts. The remaining configurations of the complex are chosen as starting models.

Next, each of these starting models is locally optimized in the 12-dimensional configuration space of a complex (S1–S6).<sup>†</sup> The minimization of the intermolecular potential  $U$ , defined with formula (2), is carried out by the method of variable metrics according to quasi-Newton<sup>20</sup> using analytical first derivatives, readily available from expressions (1) and (2) for  $U_{ij}$  and  $U$ , respectively (Figure 1 shows an example of the starting and resulting structures of the BTF–PhH complex).

The geometry of found local minima is compared to reveal and keep only unique ones, which are sorted in the order of increasing energy ( $U$ ). The locally optimal structure with the lowest energy thus obtained corresponds to the global minimum

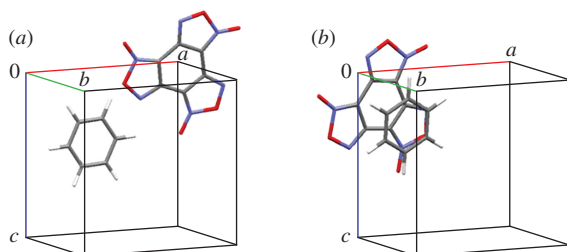


**Figure 1** (a) Generated starting model of the BTF–PhH complex and (b) the resulting structure after local optimization.

<sup>†</sup> See Online Supplementary Materials for details.

of  $U$ , which completes the global optimization process by the AAP method.

When the described approach was applied to the global optimization of the BTF–PhH complex, only one unique local minimum (readily global) was found, in which the planes of BTF and benzene molecules are parallel to each other ( $\pi$ -stacking complex). The complexation energy ( $\Delta E_{\text{AAP}}$ ) according to the AAP method was  $-9.6 \text{ kcal mol}^{-1}$  with  $-2.9$  (30%) and  $-6.7 \text{ kcal mol}^{-1}$  (70%) contributions from ES and vdW interactions, respectively.

To refine the value of  $\Delta E$ , the complex structure obtained with the AAP method was re-optimized at the B3LYP/aug-cc-pVDZ level with Grimme's D2<sup>21</sup> dispersion correction at the second stage of the two-step AAP–DFT approach. The complex remained in  $\pi$ -stacking geometry with a distance of  $\sim 3.2 \text{ \AA}$  between BTF and benzene planes (Figure 2, Table 1), while the found energy of complex formation was  $\Delta E_{\text{DFT}} = -11.9 \text{ kcal mol}^{-1}$  (calculated as the difference of ZPE-corrected energies of the complex  $E_{\text{BTF-PhH}}$  and its individual components  $E_{\text{BTF}}$  and  $E_{\text{PhH}}$ :  $\Delta E = E_{\text{BTF-PhH}} - E_{\text{BTF}} - E_{\text{PhH}}$ ).

One can find somewhat surprising that, according to an AAP-based global search, the single minimum (actually, six equivalent ones) exists on the PES of the BTF–PhH complex since several geometrically distinct minima are often located even for simpler bimolecular complexes (e.g., PhH–PhH<sup>22</sup>). Two plausible reasons could be pointed out to rationalize this result. First is the high symmetry of the components. For instance, consider the case when one H atom in benzene is replaced by D and one <sup>16</sup>O in BTF, by <sup>18</sup>O: the number of minimum-energy configurations fully analogous to that depicted in Figure 2 but nonequivalent, in principle, would be  $6 \cdot 3 = 18$ . The second reason may lie in a certain discrepancy between the interactions in BTF–benzene and pure van der Waals complexes, where electrostatics does not play an important role. While the vdW forces only aim to maximize the intermolecular contact surface area, the attractive ES interaction of  $\pi$ -electron rich benzene with BTF is possible solely in a very limited region of the configurational space due to the strong accumulation of negative charge on the electron-withdrawing periphery of the BTF molecule. The interplay of these factors probably leads to inevitable destabilization of any configuration that is far from vicinity of the found minimum point, where both ES and vdW interactions are favorable. In addition, the existence of a single unique energy minimum for the BTF–PhH complex was confirmed by the results of a DFT-based systematic PES scanning.

The above approach makes it possible to estimate the complexation energy  $\Delta E$  of bimolecular complexes in a gas

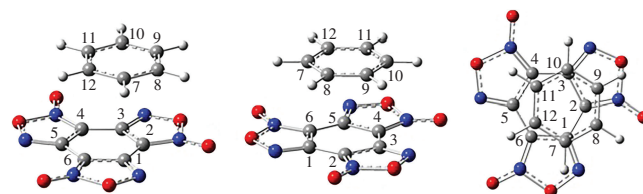


**Figure 2** Optimal geometry of the BTF–PhH complex (in three different projections).

**Table 1** The shortest intermolecular C...C contacts in the BTF–benzene complex.

Pairs of atoms <sup>a</sup>	1–7	2–8	2–9	3–10	4–11	6–12
Distance/Å	3.204	3.302	3.335	3.225	3.240	3.256

<sup>a</sup>The numbering of atoms is shown in Figure 2.

phase. Obviously, the geometry of intermolecular contacts in a crystal and respective binding energies can significantly differ from those found for an isolated complex. The approach presented below allows one to estimate the  $\Delta E$  in a crystal cluster. It is based on determining the mutual orientation of molecules of a complex, for which the cocrystal structure is simulated, followed by scanning only distances between the geometric centers of pairs of molecules to refine the energies of bimolecular interactions in a crystal by quantum-chemical calculations.

The geometries of starting components were taken from calculations by the B3LYP/aug-cc-pVDZ with Grimme's dispersion correction D2.<sup>21</sup> The point groups of molecules and charges were fixed:  $C_{3h}$  for BTF and  $D_{6h}$  for benzene. The cocrystal structure was simulated out by the AAP method<sup>18</sup> with the best model electrostatic potential for BTF and benzene obtained using the FitMEP<sup>15</sup> program analogously to the above global optimization procedure with two principle exceptions: the Evald's summation method,<sup>23</sup> instead of simple formula (2), was used to determine the crystal lattice energy, which was minimized, and the lattice parameters were optimized in the course of a global minimization process.

The crystal structure of the BTF–benzene complex is known<sup>14</sup> but not well described. Using the AAP method, we performed a structural search for the crystal packing of the test cocrystal. The modeling was carried out in 11 symmetry groups with the following statistically most probable packings of molecular crystals and cocrystals:<sup>24,25</sup>  $P2_1/c$ ,  $P2_12_12_1$ ,  $C2/c$ ,  $Cc$ ,  $P1$ ,  $P\bar{1}$ ,  $Pbca$ ,  $Pca2_1$ ,  $Pna2_1$ ,  $P2_1$ , and  $C2$ . Potential parameters of the Lennard–Jones (LJ) type ‘6–12’ were used for modeling modified<sup>26,27</sup> to better reproduce the crystal structure of polynitrogen compounds.

The global minimum **C-1** was found in the  $P2_1/c$  group (S6).<sup>†</sup> However, comparison of the simulated packings with X-ray structural data revealed that only the minimum **C-2** ( $P2_1/n$ ) corresponds to the experiment<sup>14</sup>. This fact may indicate the existence of a more stable polymorph **C-1** compared to **C-2**. The parameters of two optimal packings (reduced to 0 K) are given in Table 2. An example of complexation energy calculations for the model **C-1** is presented (S12).<sup>†</sup>

The bimolecular structures of BTF with benzene were selected from the obtained crystal packings and a molecular cluster was constructed, in which BTF molecules were surrounded by benzene molecules with intermolecular contacts between them (Figure 3, to facilitate visual perception, the benzene molecules surrounding the BTF molecule are numbered). Contacts BTF–BTF and benzene–benzene were not included in this molecular cluster.

Then, to calculate  $\Delta E$ , each pair of BTF and benzene molecules (**P1–P7**) was considered separately. The only scanned parameter was distance between the geometric centers of the molecules (**d**). In this case, the mutual orientation of the pairs of molecules remained unchanged in the course of scanning. Distances **d** were determined for a fixed mutual orientation of molecules relative to each other and were an internal coordinate relative to which scanning was performed. The shortest distances

**Table 2** Crystal packing parameters of a BTF–benzene cocrystal (1 : 1).

Space group	<i>a</i> /Å	<i>b</i> /Å	<i>c</i> /Å	$\beta$ /°	$\rho^a$ /g cm <sup>-3</sup>	$\Delta E$ /kcal mol <sup>-1</sup>
$P2_1/c$ ( <b>C-1</b> )	7.135	11.901	16.656	113.53	1.692 (0 K)	-41.73
$P2_1/n$ ( <b>C-2</b> )	15.081	6.884	14.194	119.18	1.705 (0 K)	-41.53
Exp. ( $P2_1/n$ )	15.3	7.36	13.75	116.2	1.579 (295 K)	-

<sup>a</sup> $\rho$  is the molecular density of cocrystal; Exp.: CCDC 1319292.

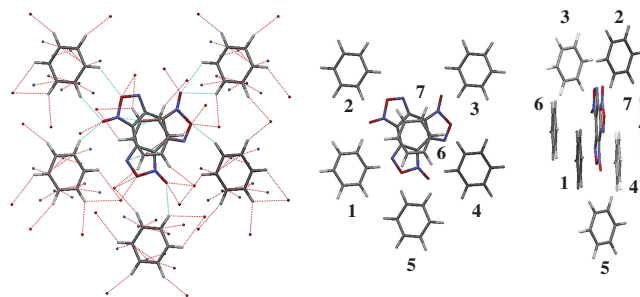


**Figure 3** The shortest (red) intermolecular contacts between the BTF molecule and surrounding benzene molecules.

**Table 3** Complexation energies of BTF–benzene (**P1–P7**) pairs for **C-1**.

The pair of BTF–benzene	<b>P1</b>	<b>P2</b>	<b>P3</b>	<b>P4</b>	<b>P5</b>	<b>P6</b>	<b>P7</b>
$d_{\text{opt}}/\text{Å}^a$	7.464	7.993	7.330	7.482	7.608	3.607	3.565
$\Delta E/\text{kcal mol}^{-1}$	-2.707	-2.238	-2.764	-2.664	-2.403	-10.885	-11.179

<sup>a</sup>Hereinafter  $d_{\text{opt}}$  is the optimized distance between geometric centers of BTF and benzene molecules.

**d** are typical for the **P6** and **P7** pairs, where benzene molecules are located above and below the plane of the BTF molecule. On average, these distances are almost two times shorter than the other contacts between molecules in the cocrystal. Next, the complexation energies [formula (1), Table 3] for the complex orientations obtained at the previous stages of scanning along the coordinate (**d**) were calculated.

It is obvious that, for pairs of BTF–benzene **P1–P5** molecules, the absolute value of  $\Delta E$  is much lower than that for pairs **P6** and **P7**. This is due to the mutual arrangement of molecules, in which the interaction of BTF with benzene molecules in pairs **P6** and **P7** is formed by the  $\pi$ -stacking type. The smallest value of  $\Delta E$  for the **C-1** model is -11.179 kcal mol<sup>-1</sup>.

For the **C-2** model (Figure 4),  $\Delta E$  (Table 4) is consistent with the known X-ray structural data.<sup>14</sup>

Tables 3 and 4 indicate that the complexation energies for the polymorphs (the predicted crystal packing **C-1** and the experimental **C-2**) are close to each other.

The cocrystallization energy was additionally estimated using the MP2/aug-cc-PVDZ, for which a crystal model was constructed. PES scanning led to a global minimum corresponding to a crystal packing that coincided with the experimental one and, accordingly, with the results of our

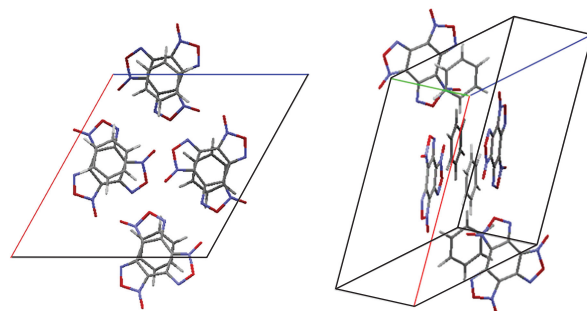


**Figure 4** Packing model of BTF–benzene in **C-2**.

**Table 4** Complexation energies of BTF–benzene (**P1–P6**) pairs for **C-2**.

The pair of BTF–benzene	<b>P1</b>	<b>P2</b>	<b>P3</b>	<b>P4</b>	<b>P5</b>	<b>P6</b>
$d_{\text{opt}}/\text{Å}$	7.298	7.829	8.152	8.092	3.443	3.534
$\Delta E/\text{kcal mol}^{-1}$	-2.848	-2.360	-2.441	-2.164	-11.657	-11.414

DFT-based PES scanning, but the cocrystallization energy was  $-21.86 \text{ kcal mol}^{-1}$ . The difference in the calculated energies is understandable: the complexation energy in the cluster is determined by comparing the energies of the complexes; therefore, it is a relative value and its estimation should be performed within the framework of the same method and basis. The MP2 method is much more computer-costly than the methods we used; therefore, its practical application to a large number of objects/models of complexes remains limited.

The approaches proposed for modeling the structure and calculating the energies of complexation in gas and crystal phases are effective. The coincidence of intermolecular interaction energies and the similarity of the most stable BTF–PhH complex structures found in the isolated and cocrystal phases is somewhat unexpected. This is probably due to a significant role of electrostatic interactions in the complex.

The paper is dedicated to the memory of N. S. Zefirov – the discoverer of scientific roads, who determined the fates of his followers.

We are grateful to Dr. A. V. Dzyabchenko and Dr. V. P. Zelenov for useful consultations and fruitful discussions and to N. M. Baraboshkin for performing a part of the calculations. The supercomputer resources were provided by the HPC centers of N. D. Zelinsky Institute of Organic Chemistry, Russian Academy of Sciences and ‘MVS100K’ of the Russian Academy of Sciences.

#### Online Supplementary Materials

Supplementary data associated with this article can be found in the online version at doi: 10.1016/j.mencom.2021.03.017.

#### References

- 1 A. Newman and R. Wenslow, *AAPS Open*, 2016, **2**, 2.
- 2 A. V. Trask, W. D. S. Motherwell and W. Jones, *Int. J. Pharm.*, 2006, **320**, 114.
- 3 H. Zhang, C. Guo, X. Wang, J. Xu, X. He, Y. Liu, X. Liu, H. Huang and J. Sun, *Cryst. Growth Des.*, 2013, **13**, 679.
- 4 Y. Tan, Z. Yang, H. Wang, H. Li, F. Nie, Y. Liu and Y. Yu, *Cryst. Growth Des.*, 2019, **19**, 4476.
- 5 J. C. Bennion, A. McBain, S. F. Son and A. J. Matzger, *Cryst. Growth Des.*, 2015, **15**, 2545.
- 6 J. Zhang and J. M. Shreeve, *CrystEngComm*, 2016, **18**, 6124.
- 7 B. Hartke, *WIREs Comput. Mol. Sci.*, 2011, **1**, 879.
- 8 D. J. Wales and M. P. Hodges, *Chem. Phys. Lett.*, 1998, **286**, 65.
- 9 J. M. C. Marques, F. B. Pereira, J. L. Llanio-Trujillo, P. E. Abreu, M. Alberti, A. Aguilar, F. Pirani and M. Bartolomei, *Philos. Trans. R. Soc., A*, 2017, **375**, doi: org/10.1098/rsta.2016.0198.
- 10 M. Bartolomei, F. Pirani and J. M. C. Marques, *J. Phys. Chem. C*, 2017, **121**, 14330.
- 11 H. Takeuchi, *J. Chem. Inf. Model.*, 2007, **47**, 104.
- 12 A. Cheung, C. S. Adjiman, P. Kolar and T. Ishikawa, *Fluid Phase Equilib.*, 2002, **194–197**, 169.
- 13 A. J. Pertsin and A. I. Kitaigorodsky, *J. Comput. Chem.*, 1987, **2**, 69.
- 14 J. C. A. Boeyens and F. H. Herbst, *J. Phys. Chem.*, 1965, **69**, 2153.
- 15 A. V. Dzyabchenko, *Russ. J. Phys. Chem. A*, 2008, **82**, 758 (*Zh. Fiz. Khim.*, 2008, **82**, 875).
- 16 M. J. Frisch, G. W. Trucks, H. B. Schlegel, G. E. Scuseria, M. A. Robb, J. R. Cheeseman, G. Scalmani, V. Barone, B. Mennucci, G. A. Petersson, H. Nakatsuji, M. Caricato, X. Li, H. P. Hratchian, A. F. Izmaylov, J. Bloino, G. Zheng, J. L. Sonnenberg, M. Hada, M. Ehara, K. Toyota, R. Fukuda, J. Hasegawa, M. Ishida, T. Nakajima, Y. Honda, O. Kitao, H. Nakai, T. Vreven, J. A. Montgomery, Jr., J. E. Peralta, F. Ogliaro, M. Bearpark, J. J. Heyd, E. Brothers, K. N. Kudin, V. N. Staroverov, T. Keith, R. Kobayashi, J. Normand, K. Raghavachari, A. Rendell, J. C. Burant, S. S. Iyengar, J. Tomasi, M. Cossi, N. Rega, J. M. Millam, M. Klene, J. E. Knox, J. B. Cross, V. Bakken, C. Adamo, J. Jaramillo, R. Gomperts, R. E. Stratmann, O. Yazyev, A. J. Austin, R. Cammi, C. Pomelli, J. W. Ochterski, R. L. Martin, K. Morokuma, V. G. Zakrzewski, G. A. Voth, P. Salvador, J. J. Dannenberg, S. Dapprich, A. D. Daniels, Ö. Farkas, J. B. Foresman, J. V. Ortiz, J. Cioslowski and D. J. Fox, *Gaussian 09, Revision D.01*, Gaussian, Wallingford, CT, 2009.
- 17 CPOSS Website, *The FIT and WILL01 Empirical ‘Repulsion-Dispersion’ Potentials*, 2020, [http://www.chem.ucl.ac.uk/cposs/dmacryl/fit\\_and\\_will01\\_empirical\\_potentials.htm](http://www.chem.ucl.ac.uk/cposs/dmacryl/fit_and_will01_empirical_potentials.htm) (accessed October 2020).
- 18 A. V. Dzyabchenko, *Russ. J. Phys. Chem. A*, 2008, **82**, 1663 (*Zh. Fiz. Khim.*, 2008, **82**, 1861).
- 19 A. V. Dzyabchenko, *Acta Crystallogr.*, 1983, **A39**, 941.
- 20 R. Fletcher, *FORTAN Subroutines for Minimization by Quasi-Newton Methods*, Harwell, England, 1972.
- 21 S. Grimme, *WIREs Comput. Mol. Sci.*, 2011, **1**, 211.
- 22 O. Bludský, M. Rubeš, P. Soldán and P. Nachtigall, *J. Chem. Phys.*, 2008, **128**, 114102.
- 23 P. Ewald, *Ann. Phys.*, 1921, **369**, 253.
- 24 V. K. Belsky, O. N. Zorkaya and P. M. Zorky, *Acta Crystallogr.*, 1995, **A51**, 473.
- 25 A. J. Cruz Cabeza, E. Pidcock, G. M. Day, W. D. S. Motherwell and W. Jones, *CrystEngComm*, 2007, **9**, 556.
- 26 D. V. Khakimov, A. V. Dzyabchenko and T. S. Pivina, *Russ. Chem. Bull., Int. Ed.*, 2020, **69**, 212 (*Izv. Akad. Nauk, Ser. Khim.*, 2020, 212).
- 27 D. V. Khakimov, A. V. Dzyabchenko and T. S. Pivina, *Propellants, Explos., Pyrotech.*, 2019, **44**, 1528.

Received: 30th November 2020; Com. 20/6383